

Optical Properties of Chiral Graphene Nanoribbons: a First Principal Study

M. Berahman^{1, 2†‡}, M. Asad¹, M. H. Sheikhi^{1, 2}

⁽¹⁾ Nanotechnology Research Institute, Shiraz University, Shiraz, Iran

⁽²⁾ School of Electrical and Compotator Engineering, Shiraz University, Shiraz, Iran

†berahman@shirazu.ac.ir

‡ Corresponding author

Abstract:

In this paper, optical properties of Chiral Graphene Nanoribbons both in longitude and transverse polarization have been studied using density functional theory calculation. It has been shown that the selection rule which have been reported before for Armchair and Zigzag Graphene Nanoribbons are no longer valid due to breaking symmetry on these new categorize of graphene nanoribbons. However, still the edge states play a critical role in optical absorption. It have been illustrated that depending on the polarization of incident beam the absorption peaks are different while it is spread in the same energy range. It is also suggested that the absorption of light is sensitive to the chiral vector on the edges and direction of the light polarization. Due to breaking symmetry in chiral graphene nanoribbons, absorption peak is changed and it would be around 1000nm, introducing a new potential of graphene nanoribbons for optoelectronic devices.

Keywords: Optical Properties, Chiral Graphene Nanoribbons, Graphene

PACS: 78.67.wj , 61.48.Gh , 73.22.Pr

1. Introduction

Graphene, the 2 dimensional structure of graphite, have shown lots of interesting Electrical [1], magnetic [2] and transport [3] properties since its synthesis in 2004 [4]. Very high electron mobility of this material, which is due to Dirac particles, makes the Graphene almost unaffected from different kind of scattering such as electron-phonon or electron- electron scatterings [1, 3]. These properties make Graphene good candidate for electrical engineering usage [5-9]. Beside these advantages, having no band gaps make Graphene noise-effective. Confining one of the dimensions of Graphene would solve this problem. These 1 dimensional allotropes of carbon are known as Graphene Nanoribbons (GNRs).

Recently, GNRs with few defects crystallography and perfect edge structures have successfully synthesized using AFM cut [10] or longitude unzipping of carbon Nanotubes (CNTs) [11-14]. GNRs have technologically promising electronic [15, 16], transport [16-20] and optical properties [21-28] due to confinement of electrons with finite width. They show very similar transport properties while have small band gaps that make them tunable by using gated configurations.

One of the most fascinating GNRs' features caused by of quantum confinement is sensitivity to edge geometrical topology [15-21]. Generally GNRs have been categorized into zigzag and Armchair edges [15-21]. However, recent success in unzipping longitude CNTs [29] showed that it would be possible to synthesis another kind of GNRs with

different edge confinement and electrical characteristics [29-31]. These new family of GNRs, have edge structure between Zigzag and Armchair, though, named as Chiral GNRs. While chiral GNRs (CGNRs) have low geometrical symmetry, Armchair and Zigzag edged are known as high symmetrical. AGNRs and ZGNRs can be classified by the number of dimer lines or zigzag chains across the ribbons width. Chiral, on the other hand, have been classified using both chiral vector and widths.

Optical properties of Armchair and Zigzag GNRs have been studied before [21-28]. In ZGNRs, most local peaks in optical spectrum have mixed polarization characteristic. This is because of the fact that for magnetic ground states, the reflection about yz plane is broken, leading to mixed polarization [27]. It has been shown before that optical transition in Z direction of ZGNRs always happen between same parity of states [22,24] and are dominant when the difference between the sub bands numbers are ± 1 [27] while y direction have direct transition [27]. On the other hand, these forbidden transitions for ZGNRs are reported elsewhere [25]. It has been reported that, owing to the symmetry of AGNRs, peaks corresponding to Z and Y polarized photons are well separated in energy [28]. Transition in Z direction is happen between odd parity states and direct band gaps [23] while it is different in other reports [27]. Different families of AGNRs can show different optical characteristic from simple dominate low energy peak in semi-metals to more transition peaks in semiconductors [25]. The absorption frequency spread from low energies (below 0.5eV) to high energies (approximately 5eV) while dominant peaks are tolerated between 0.5 to 2.5 eV. However all previous reports,

particularly in Zigzag and Armchair edges, show the importance of edge states on optical properties of GNRs [21-28]. These theoretical studies demonstrate the capability of controlling optical absorption in GNRs with width and edges and already show the potential of this material for future nano electro optic engineering devices. However, introducing chiral vector could make GNRs into new level of capability for better devices with more accurate selectivity in optical absorption spectrum.

CGNRs have interesting magnetic and electrical properties. Electrical and magnetic properties of CGNRs have been studied before using tight binding and ab initio [29-31]. It has been shown that these properties critically depend on the percentage of carbon atoms at the zigzag sites [31]. It has been reported both theoretically and experimentally that increasing width could decrease band gaps of CGNRs [29]. Also it has been demonstrated that magnetic moments and edge state energy splitting are dependent on width and chiral angle [30]. However, as far as we know, there is no report on optical properties of chiral GNRs. In this paper, optical properties of different family of CGNRs have been studied.

The rest of this paper is organized as follows. In section 2 geometrical characteristic of CGNRs have been introduced and computational method is scrutinized. Section 3 contains result and discussion of dielectric and absorption spectrum. Finally, in section 4 main results would be summarized.

2. Computational Method

Unzipping CNTs along its length direction could induce Chiral GNRs. These CGNRs could be categorized using chiral vectors (n, m) and width (w), where $n > m$ and both n and m are natural numbers and w is known as the width and is defined as the number of dimer atoms along the Armchair direction as shown in figure 1. It could be possible to use the chiral angle instead of chiral vector which defined as degree between chiral vector and zigzag direction and is calculated as follows:

$$\theta = \arcsin \sqrt{\frac{3m^2}{4(n^2 + mn + m^2)}} \quad (1)$$

In our model all the CGNRs are terminated by the Hydrogen atoms in order to omit dangling bands effects. In order to demonstrate important angles of CGNRs, (n, 1) angles use as models, where $n < 7$. The length of the carbon- carbon bond is chosen as 1.24Å and the length of carbon-hydrogen bond is 1.101Å.

The ground state electronic properties of the relaxed system obtained by performing DFT calculation, within the LDA with PZ functional for the exchange and correlation effects of the electrons as implemented in the Quantum Espresso suite of programs [32]. Optimization of each structural configuration is performed by relaxation of all atomic positions to minimize their total energies until the maximum force on any atom was less than 0.05eV/Å. The electron-ion interaction was described by the ultra soft pseudo potential, and the energy cut off was set to be 2000eV. Self consistent field procedures were performed with a convergence criterion of 10^{-5} a.u. on the energy and electron density.

To calculate the macroscopic dielectric, self consistent field used in which each electron interacts independently with a self consistent electromagnetic field [33]. Dielectric constant has been calculated based on wave function results of Hamiltonian diagonalization matrix. It defined as follow [33]:

$$\frac{1}{\varepsilon(\omega)} = \left[(1+T)^{-1} \right] \quad (2)$$

Where $\varepsilon(\omega)$ is dielectric constant within frequency region. Elements of the matrix T is $T_{k,k'}$ and defined by:

$$T_{kk'} = \frac{4\pi e^2}{(q+k)^2} \sum_{kl'} \frac{f_0(E_{k+q,l}) - f_0(E_{kl})}{E_{k+q,l'} - E_{kl} - \hbar\omega + i\Gamma} \eta_k^* \eta_{k'} \quad (3)$$

Where q is restricted to lie in the first Brillouin Zone and the K's are reciprocal lattice vectors. η_k is define as wave function for K vector which calculated using previous results from DFT. $f_0(E)$ is Fermi-Dirac destruction function. E is electron charge. Γ is small energy which would be defined. $\hbar\omega$ is energy incident beam. For long wavelength limit, it have been shown that equation (2) would be reduced to [33]

$$\varepsilon(\omega) = 1 + T_{00} + \sum_{\substack{k \\ k \neq 0}} T_{0K} \left[\frac{(1+T)^{ok}}{(1+T)^{00}} \right] \quad (4)$$

Where the superscript denotes the cofactor of the matrix elements. Equation 4 has been used in order to calculate both imaginary and real part of dielectric constant. These calculations have been done with broadening equal to 0.1eV for 8 bands in conduction band and 8 bands in valence band. Optical absorption spectrum can be calculated from dielectric constant by its famous equation [34]:

$$\alpha(\omega) \approx \frac{\omega}{\sqrt{\epsilon_2(\omega)}} \quad (5)$$

Where ϵ_2 is imaginary part of dielectric constant.

3. Results and Discussions

Figure 2 shows Bloch wave function for the (5, 1) chiral GNR in Γ and Z points in Brillouin zone. As can be seen, there is a distinct difference between valence and conduction band Bloch functions. The occupied valence band states appear to be connected along the nanoribbon direction, while the unoccupied conduction band states are more oriented across the nanoribbon. At Γ point, the states are localized towards the edges of the chiral nanoribbon. This has been shown the importance of edge states in nanoribbons are valid for CGNRs, too.

Figure 3 shows imaginary part of dielectric constant versus energy for some samples of CGNRs. M_{ij} denotes a peak in the spectrum due to a transition from the i th valence band (counted from the top) to the j th conduction band (counted from the bottom). As show in figure 3, the (1, 0) CGNR which is equal to the Zigzag GNR,

selection rule can be confirmed. As can be seen, M_{11} is important transition in all CGNRs with $n=1$, and as angle decreases this become almost the dominate peaks in spectrum. These suggest that despite of ZGNRs, direct transition is possible and important in longitude polarization.

Like ZGNRs spectrum, M_{12} and M_{21} are important in chiral, and despite of (5, 1), they create a local maximum peak around 1.2 ev. While number of Zigzag chains is increased in CGNRs, more transitions are gathered around 1.2ev so almost dominate peak of spectrum in (5,1) is created around 1.2 ev while effect if M_{12} and M_{21} is vanished.

In presence of transverse polarized light, most local and nonlocal peaks are created due to direct connection, specifically from band gaps, and in this point, chiral GNRs are most likely to Zigzag and Armchairs.

Increasing number of Zigzag chains could induce selection rules of ZGNRs in transverse direction correct for CGNRs, too. In (5, 1), or more which are not plotted here, most dominate peaks are happened in odd direct transitions. ZGNRs have no absorption under 1 ev, while CNGRs have the local peak which is created by the band gap in their energy spectrum. It could be suggested that this peak is created by local localization of wave function near armchair edges. This conclusion can be scrutinized by increasing the number of Armchair chain in CGNRS, i.e. (3, 2), which decrease the localization and completely vanish this peak in armchair edges.

By following a column of atoms in usual Zigzag GNR, which is the mother of chiral unit cells, it could be clearly seen a full Graphene (two atoms A and B) in each GNR. However in chiral GNRs there is always a missed atom compared to the AGNRs unit cell which is a perspective of breaking symmetry inside Graphene unit cell and consequently in AGNRs unit cell. These asymmetry cause activation in the bond of edge structure which caused breaking in selection rules of optic in regular GNRs in some cases but in some others, the selection rules are still correct. This is exactly the reason of disappearing separation of longitude and transverse spectrum which could be seen clearly in Armchair and Zigzag GNRs. By diverging CGNRs, either by increasing the parameter m or n of the chiral vector in proper way, The transverse symmetry along the Z direction increased, so the selection rules in ZGNRs also has rule to create the most important local peaks in CGNRs.

Figure 4, shows optical absorption spectrum of chiral GNRs versus the wavelength. The red region in figure 4 shows the visible wavelength spectrum. As illustrated, CGNRs have completely different spectrum versus Armchair and Zigzag GNRs. While Zigzag have dominate peak in low wavelength and Armchair have a very high wavelength absorption, chiral have dominant absorption peaks between these two groups. As can be seen, by increasing the angle of chiral GNRs, the dominant peaks in wavelength is slightly increased in the range from below 1000nm to above it. However, almost all CGNRs with $n=1$, show similar spectrum in visible region. This property could

be very useful in drop growth technique in optic sensors which there are no specific control on formation types of CNTs and GNRs.

4. Conclusions

In this paper, optical properties of the chiral edge Graphene Nanoribbons have been studied within DFT approximation and it have been compared to Zigzag and Armchair edge Graphene Nanoribbons. It has been shown that because of breaking yz plane symmetry in CGNRs, selection rules which were applied to zigzag Graphene Nanoribbons can not be applied and every transition depending on how this symmetry breaks is possible. It is shown that depending on the polarization of incident beam the absorption peaks are different while it is spread in the same energy bands.

Also, it have been illustrated that, like Zigzag and Armchair, in Chiral Graphene Nanoribbons, the edge states play a critical role in optical absorption. They are involved in almost all the important absorption peaks in the optical region. However, despite of Armchair and Zigzag, the peaks in Chiral GNRs are in 1000nm which demonstrates its power in optical Engineering devices in this range of wavelength.

5. References

- [1] A. H. Castro Neto, F. Guinea, N. M. R. Peres, K. S. Novoselov, and A. K. Geim The electronic properties of graphene *Rev. Mod. Phys.* 81, 109 (2009)
- [2] H. S. S. Ramakrishna Matte, K. S. Subrahmanyam and C. N. R. Rao, Novel Magnetic Properties of Graphene: Presence of Both Ferromagnetic and Antiferromagnetic Features and Other Aspects, *J. Phys. Chem. C*, 2009, 113 (23), pp 9982–9985
- [3] S. Das Sarma, Shaffique Adam, E. H. Hwang, and Enrico Rossi Electronic transport in two-dimensional graphene *Rev. Mod. Phys.* 83, 407 (2011)
- [4] K. S. Novoselov, A. K. Geim, S. V. Morozov, D. Jiang, Y. Zhang, S. V. Dubonos, I. V. Grigorieva and A. A. Firsov, Electric Field Effect in Atomically Thin Carbon Films, *Science* 22 October 2004: Vol. 306 no. 5696 pp. 666-669
- [5] Lei Liao, Yung-Chen Lin, Mingqiang Bao, Rui Cheng, Jingwei Bai, Yuan Liu, Yongquan Qu, Kang L. Wang, Yu Huang & Xiangfeng Duan High-speed graphene transistors with a self-aligned nanowire gate, *Nature* 467, 305–308
- [6] Yu-Ming Lin, Keith A. Jenkins, Alberto Valdes-Garcia, Joshua P. Small, Damon B. Farmer and Phaedon Avouris, Operation of Graphene Transistors at Gigahertz Frequencies, *Nano Lett.*, 2009, 9 (1), pp 422–426
- [7] G. Liu, W. Stillman, S. Rumyantsev, Q. Shao, M. Shur, and A. A. Balandin Low-frequency electronic noise in the double-gate single-layer graphene transistors, *Appl. Phys. Lett.* 95, 033103 (2009)
- [8] Roman Sordan, Floriano Traversi, and Valeria Russo, Logic gates with a single graphene transistor, *Appl. Phys. Lett.* 94, 073305 (2009)
- [9] Frank Schwierz Graphene transistors, *Nature Nanotechnology*, 5, 487–496 (2010)
- [10] R. K. Puddy, P. H. Scard, D. Tyndall, M. R. Connolly, C. G. Smith, G. A. C. Jones, A. Lombardo, A. C. Ferrari, and M. R. Buitelaar Atomic force microscope nanolithography of graphene: Cuts, pseudocuts, and tip current measurements, *Appl. Phys. Lett.* 98, 133120 (2011)
- [11] Dmitry V. Kosynkin, Amanda L. Higginbotham, Alexander Sinitskii, Jay R. Lomeda, Ayrat Dimiev, B. Katherine Price & James M. Tour Longitudinal unzipping of carbon nanotubes to form graphene nanoribbons,
- [12] Alexandr V. Talyzin, Serhiy Luzan, Ilya V. Anoshkin, Albert G. Nasibulin, Hua Jiang, Esko I. Kauppinen, Valery M. Mikoushkin, Vladimir V. Shnitov, Dmitry E. Marchenko and Dag

Noréus, Hydrogenation, Purification, and Unzipping of Carbon Nanotubes by Reaction with Molecular Hydrogen: Road to Graphane Nanoribbons, *ACS Nano*, 2011, 5 (6), pp 5132–5140

[13] Liying Jiao, Li Zhang, Xinran Wang, Georgi Diankov & Hongjie Dai Narrow graphene nanoribbons from carbon nanotubes, *Nature* 458, 877-880 (16 April 2009)

[14] Liming Xie, Hailiang Wang, Chuanhong Jin, Xinran Wang, Liying Jiao, Kazu Suenaga, and Hongjie Dai Graphene Nanoribbons from Unzipped Carbon Nanotubes: Atomic Structures, Raman Spectroscopy, and Electrical Properties, *J. Am. Chem. Soc.* 2011, 133, 10394–10397

[15] Melinda Y. Han, Barbaros Özyilmaz, Yuanbo Zhang, and Philip Kim Energy Band-Gap Engineering of Graphene Nanoribbons, *Phys. Rev. Lett.* 98, 206805 (2007)

[16] Katsunori Wakabayashi, Yositake Takane, Masayuki Yamamoto and Manfred Sigrist Electronic transport properties of graphene nanoribbons *New J. Phys.* 11 095016 (2009)

[17] Cheng Ling, Gabriel Setzler, Ming-Wei Lin, Kulwinder Singh Dhindsa, Jin Jin, Hyeun Joong Yoon, Seung Soo Kim, Mark Ming-Cheng Cheng, Noppi Widjaja and Zhixian Zhou, Electrical transport properties of graphene nanoribbons produced from sonicating graphite in solution, *Nanotechnology* 22 325201 (2011)

[18] Katsunori Wakabayashi, Yositake Takane, Masayuki Yamamoto, Manfred Sigrist Edge effect on electronic transport properties of graphene nanoribbons and presence of perfectly conducting channel, *Carbon* Volume 47, Issue 1, January 2009, Pages 124–137

[19] V. A. Rigo, T. B. Martins, Antonio J. R. da Silva, A. Fazzio, and R. H. Miwa Electronic, structural, and transport properties of Ni-doped graphene nanoribbons, *Phys. Rev. B* 79, 075435 (2009)

[20] Denis A. Areshkin, Daniel Gunlycke, and Carter T. White Ballistic Transport in Graphene Nanostrips in the Presence of Disorder: Importance of Edge Effects *Nano Lett.*, 2007, 7 (1), pp 204–210

[21] M Berahman, M. H. Sheikhi, Optical Excitations of Finite Length Graphene Nanoribbons, *J. Comput. and Theor. Nanosci.* , Volume 8, Number 1, January 2011 , pp. 90-96(7)

[22] H. Hsu and L.E. Reichl, Selection rule for the optical absorption of graphene nanoribbons, *Physical Review B* 76, 045418 (2007)

[23] Li Yang, Marvin L. Cohen, and Steven G. Louie, Excitonic Effects in the Optical Spectra of Graphene Nanoribbons, *Nano Lett.*, 2007, 7 (10), pp 3112–3115

[24] Jhao-Ying Wu , Li-Han Chen , To-Sing Li , and Ming-Fa Lin, Optical properties of graphene nanoribbon in a spatially modulated magnetic field, *Appl. Phys. Lett.* 97, 031114 (2010)

- [25] Wenhui Liao, Guanghui Zhou, and Fu Xi, Optical properties for armchair-edge graphene nanoribbons, *J. Appl. Phys.* 104, 126105 (2008)
- [26] Deborah Prezzi, Daniele Varsano, Alice Ruini, Andrea Marini, and Elisa Molinari, Optical properties of graphene nanoribbons: The role of many-body effects, *Phys. Rev. B* 77, 041404(R) (2008)
- [27] Ken-ichi Sasaki, Keiko Kato, Yasuhiro Tokura, Katsuya Oguri, and Tetsuomi Sogawa, Theory of optical transitions in graphene nanoribbons, *Phys. Rev. B* 84, 085458 (2011)
- [28] Kondayya Gundra and Alok Shukla, Theory of the electro-optical properties of graphene nanoribbons, *Phys. Rev. B* 83, 075413 (2011)
- [29] Chenggang Tao, Liying Jiao, Oleg V. Yazyev, Yen-Chia Chen, Juanjuan Feng, Xiaowei Zhang, Rodrigo B. Capaz, James M. Tour, Alex Zettl, Steven G. Louie, Hongjie Dai, Michael F. Crommie, Spatially resolving edge states of chiral graphene nanoribbons, *Nature Physics* 7, 616–620 (2011)
- [30] Oleg V. Yazyev, Rodrigo B. Capaz, and Steven G. Louie, Theory of magnetic edge states in chiral graphene nanoribbons, *Phys. Rev. B* 84, 115406 (2011)
- [31] Lili Sun, Peng Wei, Jianhua Wei, Stefano Sanvito and Shimin Hou, From zigzag to armchair: the energetic stability, electronic and magnetic properties of chiral graphene nanoribbons with hydrogen-terminated edges, *J. Phys.: Condens. Matter* 23 425301
- [32] Paolo Giannozzi, Stefano Baroni, Nicola Bonini, Matteo Calandra, Roberto Car, Carlo Cavazzoni, Davide Ceresoli, Guido L Chiarotti, Matteo Cococcioni, Ismaila Dabo, Andrea Dal Corso, Stefano de Gironcoli, Stefano Fabris, Guido Fratesi, Ralph Gebauer, Uwe Gerstmann, Christos Gougoussis, Anton Kokalj, Michele Lazzeri, Layla Martin-Samos, Nicola Marzari, Francesco Mauri, Riccardo Mazzarello, Stefano Paolini, Alfredo Pasquarello, Lorenzo Paulatto, Carlo Sbraccia, Sandro Scandolo, Gabriele Sclauzero, Ari P Seitsonen, Alexander Smogunov, Paolo Umari and Renata M Wentzcovitch, QUANTUM ESPRESSO: a modular and open-source software project for quantum simulations of materials, *J. Phys.: Condens. Matter* 21 395502 (2009)
- [33] N. Wiser, Dielectric Constant with Local Field Effects Included *Phys. Rev* 129, 62 (1963)
- [34] N. Peyghambarian, S.W. Koch, A.Mysyrowicz, Introduction to Semiconductor Optics, Prentice Hall (1993) page 56

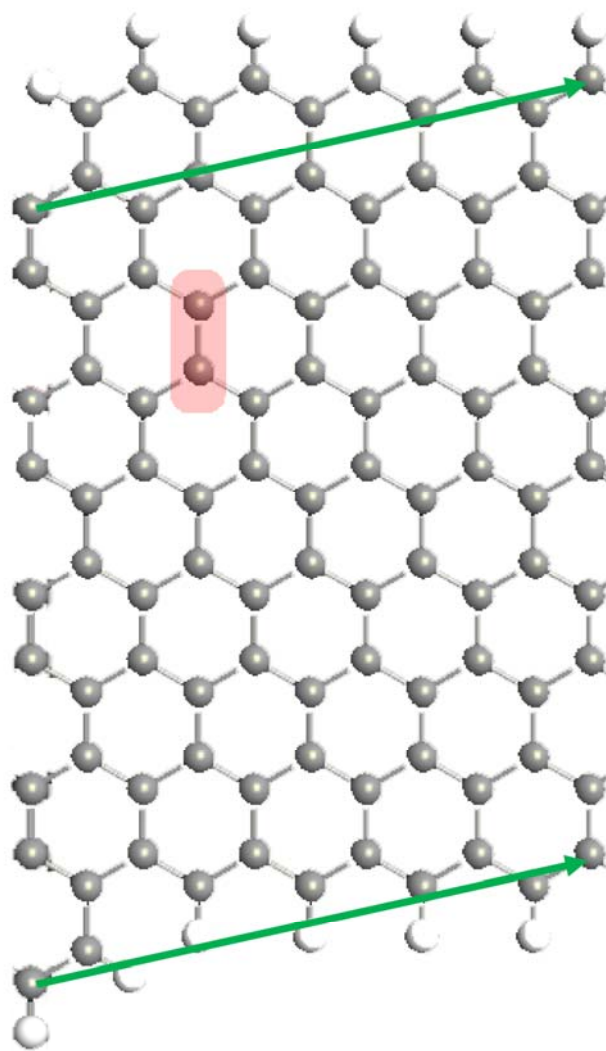


Figure 1: (5,1) Chiral Graphene Nanoribbons. Gray circles are Carbon atoms and white circles are Hydrogen atoms. The Green vector is Chiral Vector. The red area illustrates atoms in the unit cell of Graphene.

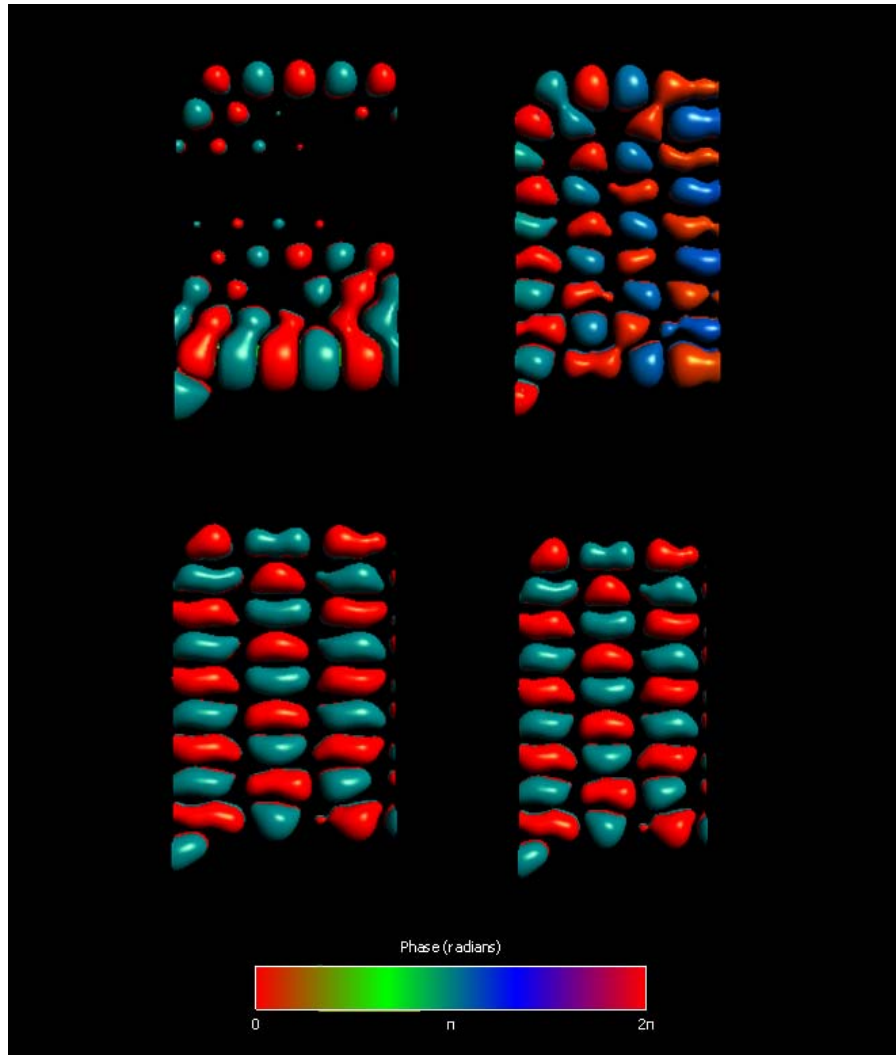


Figure 2: From left to right the Γ point and the Z point Bloch wave function of (5, 1) Chiral Graphene Nanoribbon. The top and bottom rows display the conduction and valance band, respectively.

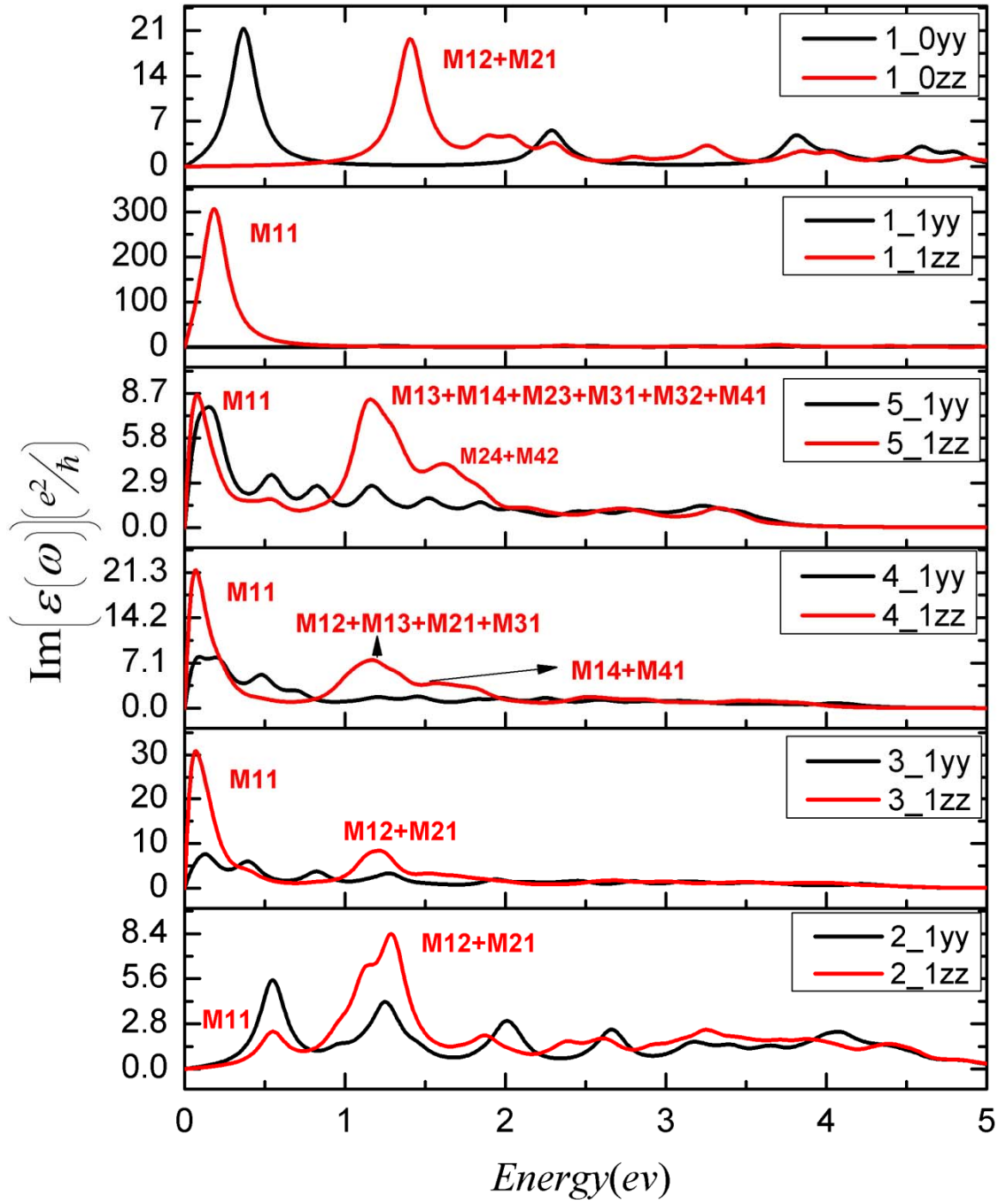


Figure 3: Imaginary part of dielectric constant versus Energy for different kind of Chiral Graphene Nanoribbons. Red curves demonstrate Z polarization of incident beam and Black curves illustrate Y polarization of incident beam

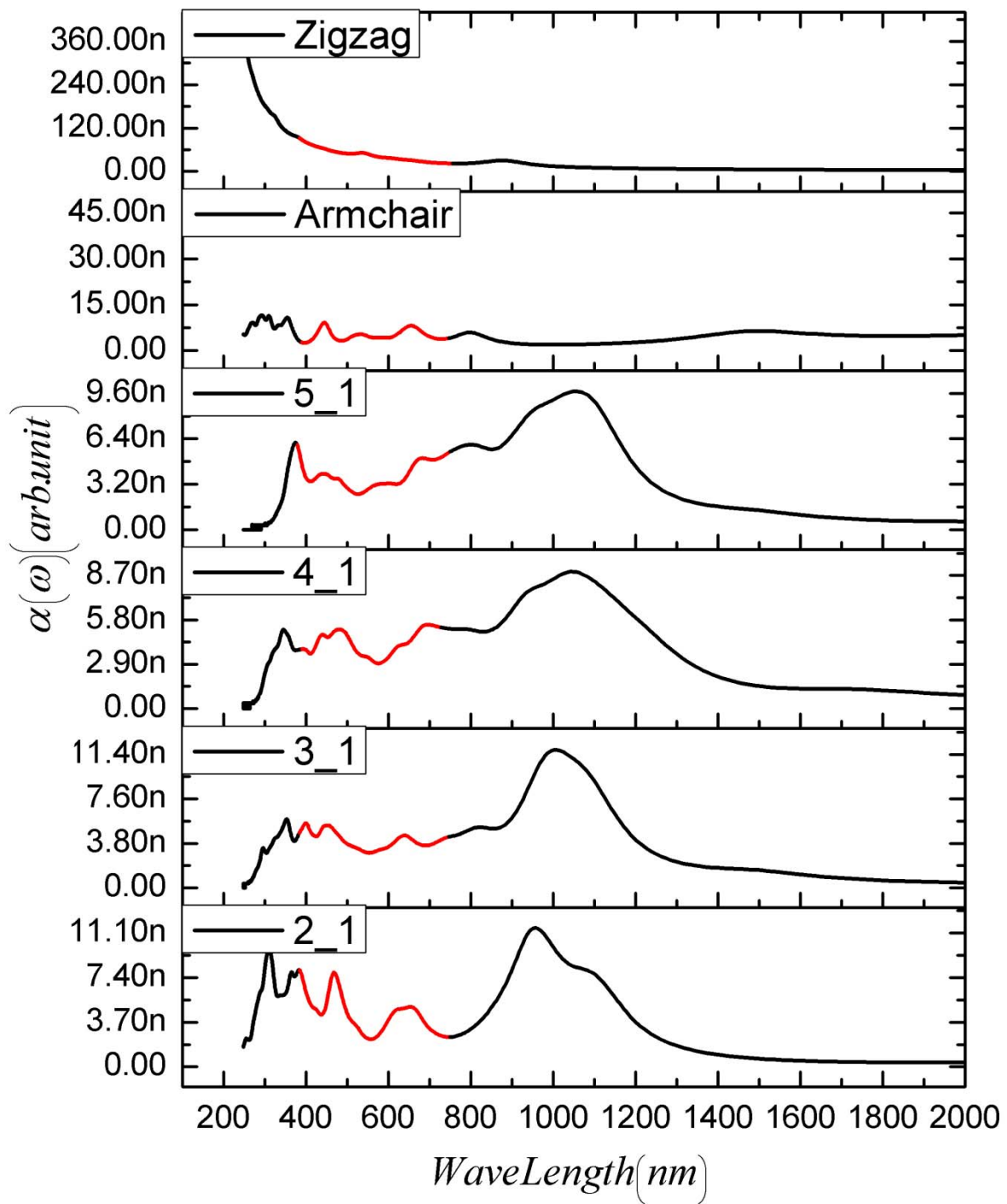


Figure 4: Optical Absorption versus Wavelength for different Chiral Graphene Nanoribbons. The Red Area illustrates visible spectrum range.